*J. Chem. Sci.* Vol. 125, No. 1, January 2013, pp. 193–202. 

# Preparation of amphiphilic block copolymer containing triazene moieties and fluorescence study

EMIL C BURUIANA*, ANDREEA L CHIBAC, VIOLETA MELINTE and TINCA BURUIANA
'Petru Poni' Institute of Macromolecular Chemistry, 41 A Grigore Ghica Voda Alley, 700487, Iasi, Romania
e-mail: emilbur@icmpp.ro

MS received 23 January 2012; revised 25 April 2012; accepted 11 May 2012

**Abstract.** The present study describes the synthesis via microwave accelerated reversible addition-fragmentation chain transfer (RAFT) polymerization of an amphiphilic block copolymer *poly(acrylic acid)-b-poly(dodecylacrylamide-co-1-(phenyl)-3-(2-methacryloyloxyethyl carbamoyloxyethyl)-3-methyltriazene-1) [PAA-b-(PDA-co-PUMA-T)]*. The structure and the chemical composition of the block copolymer were confirmed by spectral/thermal analysis. The photoreactivity of the triazene sequences from *PAA-b-(PDA-co-PUMA-T)* was quantified by UV/vis irradiation in chloroform/dimethylformamide solutions and in thin film, indicating that the solvent polarity modifies with an order of magnitude the rate constant values. The lower rate constant in film state ($k_{film} = 1.3 \times 10^{-3}$ s$^{-1}$), shows that the higher mobility of polymeric chains in solution allow a more rapid orientation, favourable to the triazene bond cleavage. The capability of block copolymer to form micelles in aqueous environment and implicitly, its critical micelle concentration (CMC) was evidenced through fluorescence measurements using pyrene probe ($10^{-6}$ M), the CMC value being of $4.64 \times 10^{-3}$ g L$^{-1}$ PAA-*b*-(PDA-*co*-PUMA-T) ($3.27 \times 10^{-7}$ M). Experiments of fluorescence quenching with various metal cations ($UO_2^{2+}$, $Fe^{2+}$, $Fe^{3+}$, $Ni^{2+}$, $Cu^{2+}$, $Co^{2+}$, $Pb^{2+}$ and $Hg^{2+}$) suggested that such a block copolymer could find applications as fluorescence-based chemosensor for the detection of iron cations in homogeneous organic solutions or aqueous environments by thin films.

**Keywords.** Amphiphilic block copolymer; RAFT polymerization; photodecomposition; fluorescence; chemosensor.

## 1. Introduction

In the recent literature, the design of polymers carrying photoresponsive sequences constitute an appropriate and useful tool to create materials with broad applicability in the development of optical data recording materials,[1] liquid crystals,[2] nonlinear optics[3] or photoresists for microlithography purposes.[4] From the perspective of the photosensitivity characteristics, polymers containing triazene groups ($-N=N-N<$) have been identified as the most promising candidates for ablation experiments, since they show an intensive absorption maximum around 300 nm and may undergo a selective breaking of the polymer chains at well-defined positions, when they are irradiated with a suitable wavelength. Until now, different triazene polymers like polyesters, polysulphides, and polytriazenes have been reported in the literature.[5–7] In this regard, our contribution in the synthesis of novel triazene polyurethanes and copolyacrylates that combine the sensitivity of the triazene structure with an almost unlimited structural variability offered by the macromolecular chemistry of these polymers should be mentioned.[8–11] Moreover, in recent publications, the important attribute of the triazene copolymers to emit a strong fluorescence with a maximum around 400 nm was confirmed, feature of interest in chemosensor applications for the detection of some metal ions.[12,13]

Meanwhile, the modern developments in reversible addition-fragmentation chain transfer (RAFT) polymerization have proved that this is one of the most versatile methods of controlled radical polymerization, successfully employed in preparing complex macromolecular architectures such as linear block copolymers, star and brush polymers, dendrimers.[14–16] Usually, RAFT polymerization is a living polymerization that yields polymers with a low polydispersity index and a predetermined molecular weight[16] and facilitates the controlled polymerization of a wide range of non-functional monomers under a great variability of experimental conditions.[17] Given the remarkable features of RAFT, varieties of block copolymers[18] including hydrophilic-hydrophobic ones were synthesized and characterized.[19–22] The amphiphilic block copolymers are particularly interesting due to their notable ability to self-assemble in selective solvents with formation of

nano- or micrometric aggregates,[23,24] such as spherical or elongated micelles, rods, vesicles (also, called polymersomes), or other morphologies with different well-organized supramolecular structures.[25,26] Among these, polymeric micelles self-assembled from amphiphilic block copolymers into an aqueous phase have attracted much attention, owing to their unique morphological characteristics, and especially, to their potential applicability in the area of drug delivery.[27–29]

To further extend the range of the responsive materials, the microwave-assisted polymerization was also employed, since this special heating energy could greatly shorten the synthesis time and can induce enhanced reaction rates and yields, high purity, and better selectivity, in comparison with the reactions performed with conventional heating.[30–32] Under optimized conditions, reactants directly absorb microwave irradiation, while in the case of typical conventional heating (e.g., with an oil bath) the energy is transferred, often via solvent, by thermal conduction. This methodology was successfully utilized in the synthesis through RAFT polymerization combined with microwave irradiation of some polymeric materials derived from commercial acrylic monomers such as acrylamides, styrene, methacrylic acid, etc.[33–36] However, to the best of our knowledge, these reactions have not yet been used in triazeno-polymer synthesis.

In the present study, we report the synthesis through microwave-accelerated RAFT polymerization of an amphiphilic block copolymer bearing triazene photosensitive moieties, in which the first block of poly(acrylic acid) with end dithiobenzoate group behaves as macro chain transfer agent to control the polymerization of the monomers that construct the second block. The structures of RAFT agent and block copolymer *poly(acrylic acid)-b-poly(dodecylacrylamide-co-1-(phenyl)-3-(2-methacryloyloxyethylcarbamoyloxyethyl)-3-methyltriazene-1) [PAA-b-(PDA-co-PUMA-T)]* together with the photosensitivity and sensing ability of the macromolecular assembly are investigated here.

## 2. Experimental

### 2.1 *Materials*

Bromobenzene, magnesium, carbon disulphide, benzyl bromide, acrylic acid, 1,1′–azobis(cyclohexanecarbonitrile) (ABCN), dodecylamine, acryloyl chloride, triethylamine, tetrahydrofuran (THF), diethyl ether, dioxane, chloroform ($CHCl_3$), dimethylformamide (DMF) were used as received (Aldrich) without any purification.

### 2.2 *Synthesis of the poly(acrylic acid) macro-RAFT agent (macroPAA)*

Dodecylacrylamide monomer (DA), triazene urethane methacrylate (UMA-T) and benzyl dithiobenzoate (BDTB) were obtained as previously reported.[11,37,38] The macroPAA was prepared through the RAFT polymerization of acrylic acid (9 g, 125 mmol) in dioxane, in the presence of benzyl dithiobenzoate (0.244 g, 1 mmol) and 1,1′–azobis (cyclohexanecarbonitrile) (0.124 g, 0.5 mmol) used as chain transfer agent and initiator, respectively. The mixture was reacted under microwave irradiation at 100 °C for 90 min, under purified nitrogen. The resulting polymer was purified by precipitation in diethyl ether, dried in an oven at 60 °C for 24 h and then under reduced pressure. The yield of the macroPAA was 79%.

FTIR (KBr, $cm^{-1}$): 3230 (O–H from carboxyl); 2968–2931 ($CH_2$); 1740 (C=O bounded); 1702 (C=O unbounded); 1457 (aromatic); 1257, 1159 and 1115 (C–O); 1044 (C=S).

### 2.3 *Microwave RAFT block copolymerization of macroPAA with DA and UMA-T*

RAFT block copolymerization of macroPAA with DA and UMA-T was conducted as follows: 1 g macroPAA (0.1342 mmol, $M_n = 7450$), 0.017 g (0.0671 mmol) 1,1′–azobis (cyclohexanecarbonitrile), 1.44 g (6.04 mmol) DA, 0.22 g (0.671 mmol) UMA-T and dioxane (5 mL) were sealed in a vial equipped with a magnetic stirrer bar. After purging with nitrogen, the sealed vial was placed in the microwave at 100 °C for 90 min. The obtained solution was concentrated under reduced pressure, and subsequently, the block copolymer PAA-*b*-(PDA-*co*-PUMA-T) was purified by precipitation in diethyl ether, dried at 60 °C for 24 h, and then under reduced pressure. The yield of PAA-*b*-(PDA-*co*-PUMA-T) was 72.6%.

FTIR (KBr, $cm^{-1}$): 3500–3312 (O–H from carboxyl and NH urethane); 2850–2940 ($CH_2$); 1734 (C=O); 1648 (amide I); 1550 (amide II); 1467 (aromatic); 1378 (−N=N−N<); 1252 and 1168 (C–O); 1044 (C=S).

### 2.4 *Measurements*

The structures of all synthesized derivatives were verified by $^1$H NMR, FTIR, and UV spectroscopy. $^1$H NMR spectra were recorded on a Bruker Avance DRX 400 MHz spectrometer in $D_2O$, $CDCl_3$ and DMSO at room temperature. FTIR spectra were recorded using a Bruker Vertex 70 FT-IR instrument. The UV absorption

spectra were measured with a Specord 200 spectrophotometer in $CHCl_3$/DMF solution and in thin film. UV irradiations were performed using a 500 W high-pressure mercury lamp without wavelength selection, at room temperature. The molecular weight of polymers was determined by gel permeation chromatography (GPC) measurements performed on a Polymer Laboratory MD-950 apparatus equipped with an evaporative mass detector and two PL gel 5 μm columns using THF as solvent and polystyrene standards for calibration. The thermal stability of macroinitiator and block copolymer was evaluated by thermogravimetric analysis (TGA) on a STA 449 F1 Jupiter apparatus (Netzsch-Germany) in the temperature range of 25–600°C under static air atmosphere, at a heating rate of 10 °C·min$^{-1}$. Sample weights in the range 5–10 mg, and $Al_2O_3$ crucibles were used. The Netzsch Thermokinetics-A software module for kinetic analysis of thermal measurements program allow us to process the initial TG and differential thermogravimetric (DTG) curves. Polymer surface morphology was examined by means of atomic force microscopic (AFM) technique using a SOLVER PRO–M AFM. The polymeric films for AFM experiment were prepared using a spin coater Model WS-400B-6NPP/LITE/10K from Laurel Tech at 3000 rpm, the images being registered in different points of the sample to check their reproducibility. The fluorescence intensity measurements were carried out with a Perkin–Elmer LS 55 spectrophotometer at room temperature in DMF solution and in thin film. Excitation wavelength was 320 nm and the emission spectra were recorded over a range of 330–600 nm. For the critical micelle concentration determination by fluorescence measurements, a set of aqueous solutions of block copolymer with concentrations varying between $5 \times 10^{-5}$ g/L and $2.6 \times 10^{-2}$ g/L were prepared. In each block copolymer sample, a solution of pyrene solubilized in THF was added, so that the pyrene concentration in aqueous solution after evaporating THF to be around $5 \times 10^{-6}$ M. The average size of the PAA-*b*-(PDA-*co*-PUMA-T) micelles was measured by dynamic light scattering (DLS) method, employing Zetasizer Nano Zs equipment.

## 3. Results and discussion

### 3.1 *Synthesis and spectral characterization*

For this study, benzyl dithiobenzoate RAFT agent, designated BDTB was firstly synthesized according to a technique reported by Chong and co-workers.[38] The RAFT polymerization of acrylic acid (AA) in the presence of BDTB and 1,1′–azobis (cyclohexanecarbonitrile) as initiator, under microwave irradiation is outlined in scheme 1. The structure of the formed macroPAA was confirmed by spectroscopic techniques, thus in the $^1$H NMR spectrum of macroPAA (figure 1a) the resonance signals attributed to the aromatic protons (8.1–7.2 ppm), methyne protons linked to the carboxyl groups (2.42 ppm), and to the methylene protons from the aliphatic chain (1.95 to 1.63 ppm) can be identified. The molecular weight of macroPAA determined by $^1$H NMR analysis was estimated taking into consideration the integral ratio of aromatic protons resulting from the BDTB to that of methyne protons (-$CH_2$-C*H*(COOH)) that give the signal at 2.42 ppm, the calculated number average molecular weight of macroPAA being 7450 g/mol (100 monomer units). This result is in good agreement with the molecular weight determined by GPC when an $M_w$ of 9500 g mol$^{-1}$ and a polydispersity index of 1.2 were obtained. MacroPAA is soluble in common solvents such as $H_2O$, $CHCl_3$, THF, DMF and DMSO and has good film-forming abilities.

The novel fluorescent diblock copolymer PAA-*b*-(PDA-*co*-PUMA-T) consisting of hydrophilic poly (acrylic acid) part and hydrophobic block composed of PDA-*co*-PUMA-T random copolymer, was further prepared via RAFT controlled radical polymerization of the monomer mixture based on DA and UMA-T using macroPAA and 1,1′–azobis (cyclohexanecarbonitrile) as macromolecular chain transfer agent and initiator, respectively (scheme 1b). $^1$H NMR analysis of the PAA-*b*-(PDA-*co*-PUMA-T) block copolymer (figure 1b) indicated the appearance of a resonance signal attributed to the carboxylic proton coming from the COOH group (12.4 ppm). Other signals were assigned to the aromatic protons (8.04–7.16 ppm), methylene protons from ester (4.17 ppm), methylene protons linked to urethane NH/amide (3.5–3.1 ppm), methyne protons (2.22 ppm), methylene and methyl protons from the backbone (1.75–1.39 ppm), and to methylene/methyl protons from DA (1.25 ppm; 0.86 ppm). From these, we deduced that the RAFT agent was clearly attached to the polymer backbone. Based on $^1$H NMR spectrum analysis, the structural composition of the synthesized block copolymer was calculated by comparing the integrals of methyl protons of DA at 0.86 ppm, methyne protons of AA at 2.22 ppm, methylene protons of UMA-T at 4.16 ppm and that of the aromatic protons from BDTB at 8.1–7.2 ppm. Accordingly, the mol percent of monomer units in the block copolymer was found to be 79.36:16.66:3.97 (AA:DA:UMA-T). The molecular weight of the block copolymer calculated from the $^1$H NMR spectrum ($M_n$)

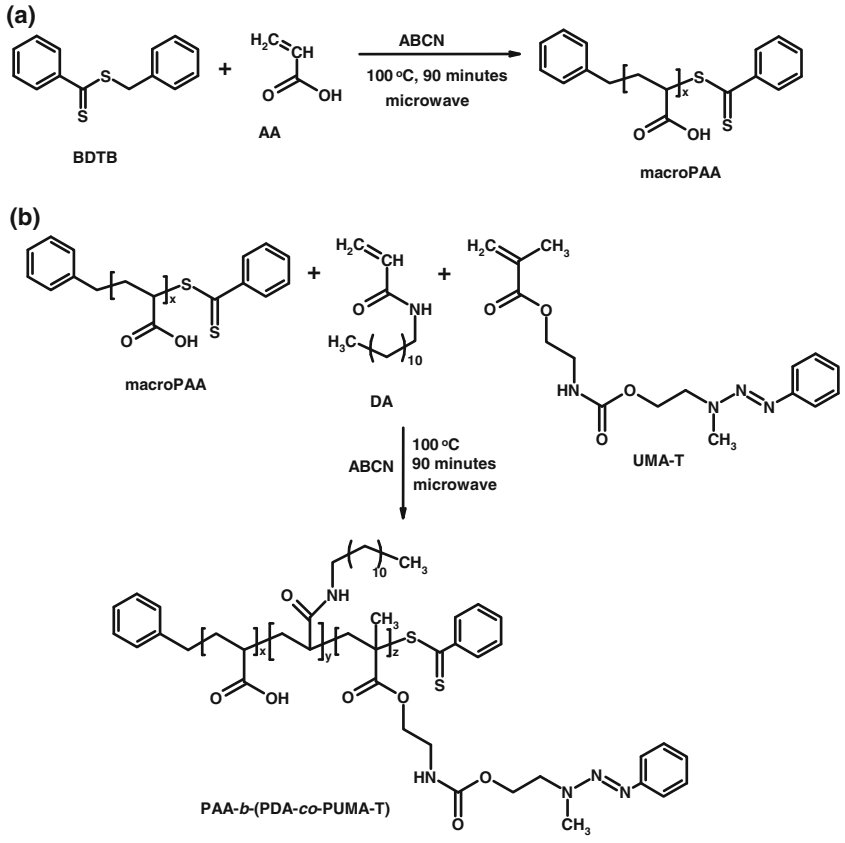


**Scheme 1.** Synthesis of the macro-RAFT agent (macroPAA) (**a**) and of the amphiphilic block copolymer PAA-*b*-(PDA-*co*-PUMA-T) (**b**).

was of 14100 g/mol, while that determined by GPC was around of 17200 g/mol (PI = 1.22). PAA-*b*-(PDA-*co*-PUMA-T) is soluble in THF, DMF, and $CHCl_3$, and has good film-forming properties.

### 3.2 *Thermal behaviour and surface morphology*

The thermal properties of both polymers were studied by thermogravimetric analysis (TGA), the resulting traces revealing a two-stage degradation pattern (figure 2). In the case of macroPAA agent, the first stage of thermal decomposition ($T_{onset}$) starts around 163°C and is mainly attributed to the decarboxylation of the poly(acrylic acid) (weight loss 44.25 wt. %), whereas in the PAA-*b*-(PDA-*co*-PUMA-T) this begins at about 171°C and is associated with the break of triazene moieties followed by the release of nitrogen and aromatic fragments together with the decarboxylation of

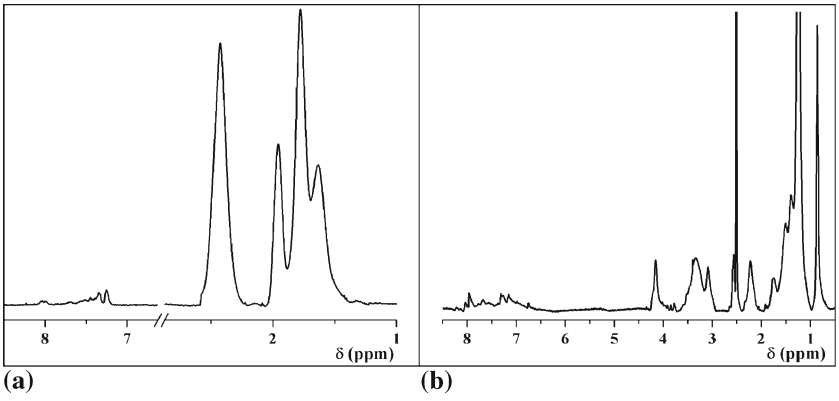


**Figure 1.** $^1$H NMR spectra of macroPAA in $D_2O$ (**a**) and of PAA-*b*-(PDA-*co*-PUMA-T) in DMSO (**b**).

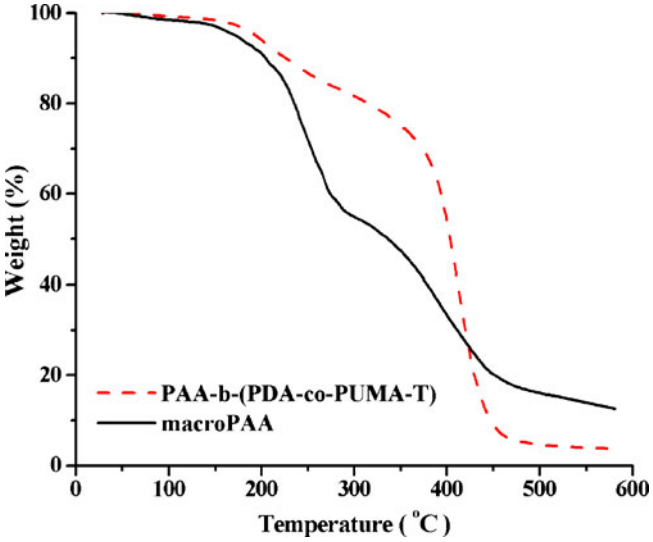


**Figure 2.** Thermogravimetric decomposition pathway for the macroPAA and block copolymer measured by TGA analysis.

poly(acrylic acid) sequences (weight loss 17.8 wt.%). The second step of thermal degradation occurs after 320°C and is ascribed to the advanced thermal degradation of the polymer chains. In both cases, the final decomposition temperatures at which this process is ended ($T_{endset}$) were around 465°C.

Surface morphology of the above polymers in thin films was visualized by atomic force microscopy (AFM) in tapping mode, the samples being prepared by spin coating on silicon wafers. The recorded 3D micrographs for the macroPAA (figure 3a) and the PAA-*b*-(PDA-*co*-PUMA-T) diblock copolymer obtained by RAFT technique (figure 3b) suggested a homogeneous morphology of the polymers surface. It can be observed that the macroPAA has a smooth surface, whereas the PAA-*b*-(PDA-*co*-PUMA-T) surface contains small aggregates of about 43 nm in height. Obviously, the existence of small aggregates could be associated to the low crystallinity extent of the block copolymer distributed into an amorphous matrix. The values of average roughness calculated for the above polymers are 2.54 nm for macroPAA and 2.31 nm for PAA-*b*-(PDA-*co*-PUMA-T), evidencing that the hydrophobic block had no significant effect on the morphology.

### 3.3 *Photobehaviour studies of block copolymer containing triazene moieties*

To investigate the photolability of the triazene structure, the progress of the photodecomposition reaction of the block copolymer by an exhaustive irradiation with a high-pressure mercury lamp was monitored via UV/vis spectroscopy. We first examined the photochemical behaviour of the block copolymer in $CHCl_3$ solution, when a gradual decrease of the absorption maximum intensity at 280 nm with irradiation time took place, suggesting the irreversible photodecomposition of the triazene unit from block copolymer (figure 4a). As can be noticed from the figure, the photodecomposition of the triazene groups was accomplished in the first 75 s of irradiation. After this period the photoprocess attains a stationary phase (up to 200 s of UV irradiation), when the absorption maximum intensity shows a modest decrease that confirms the complete photolysis of triazene sequences from the solution within 75 s of UV irradiation. The spectral changes were expressed through the photolysis rate values, for which the rate constant k was determined according to equation:

$$\ln (A_0/A_t) = kt,$$

where, $A_0$ and $A_t$ are the values of the absorbance at times $t_0$ and $t$, respectively, and $k$ is the rate constant. Hence, for PAA-*b*-(PDA-*co*-PUMA-T) block copolymer in chloroform solution the calculated rate constant is $k = 2.3 \times 10^{-2}\ s^{-1}$ (figure 4b). To monitor the influence of the solvent polarity on the triazene photolysis parameters, the same photodecomposition study was performed in DMF solution, a common polar solvent, where the rate constant ($k = 3.2 \times 10^{-3}\ s^{-1}$) was lower with an order of magnitude than that found in the nonpolar solvent $CHCl_3$. It can be assumed that, according to our previous results[9,39] the polar solvent induces an apparent stabilization of the formed radicals through the

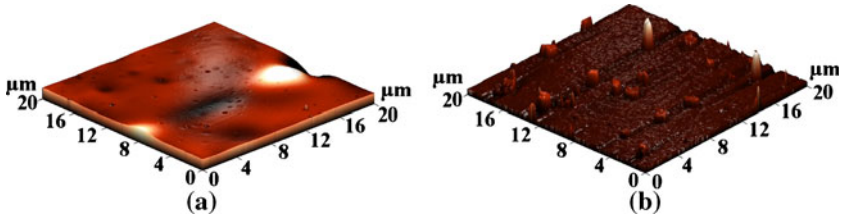


**Figure 3.** AFM images for macroPAA (**a**) and PAA-*b*-(PDA-*co*-PUMA-T) (**b**).

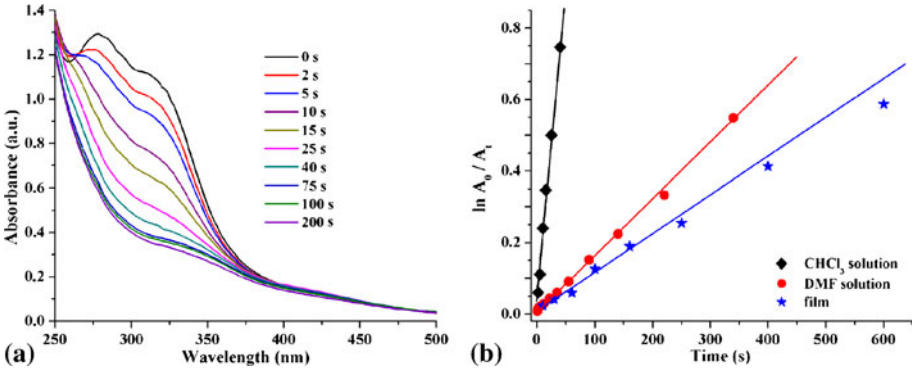


**Figure 4.** The UV photodecomposition of triazene block copolymer in chloroform solution (**a**) and the kinetic estimation of the photolysis (**b**).

'cage effect', thus favouring their recombination. Given the importance of film state photochemical behaviour for the triazene moieties in dry etching applications, a block copolymer film was subjected to UV irradiation to establish its ability to function as photolithographic material. The photolytic degradation of triazene moieties into a thin film of PAA-*b*-(PDA-*co*-PUMA-T) proceeds in 900 s with a rate constant $k = 1.3 \times 10^{-3}\ s^{-1}$. A comparison of the obtained results shows that the photosensitivity of triazene groups is better in polymer solution than in film state (although the polar solvents tend to stabilize the radicals formed upon triazene photolysis), due to the higher mobility of the polymeric chains in solution, that allow a more rapid orientation of them influencing the triazene bond cleavage.

Further evidence in supporting the photodecomposition of triazene group is an enhancement of the fluorescence intensity after UV irradiation of PAA-*b*-(PDA-*co*-PUMA-T) in solution and thin film (not shown here). The increase in the fluorescence intensity of about 3 times after 200 s irradiation of the polymer solution suggested that the products formed through a recombination of diazenyl radicals emit fluorescence. A similar effect was also observed in thin film, but in this case, the fluorescence enhancement was not evident as in the polymer solution. From this experiment, it is obvious that the triazene moiety (>*N*−*N*=*N*−) is responsible for emission maximum.[12]

### 3.4 *Critical micelle concentration (CMC) in aqueous solution*

As mentioned above, amphiphilic block copolymers can create micelle-like structures through a self-assembling process in aqueous solution.[40] Consequently, the amphiphilic nature of the block copolymer with hydrophilic PAA sequences and hydrophobic PDA-*co*-PUMA-T block provides a good opportunity to inspect the formation of micelles in water. The most frequently used method to assess the critical micelle concentration (CMC) value for copolymer solutions is that based on fluorescence measurements.[41,42] Regarding the CMC evaluation for our block copolymer PAA-*b*-(PDA-*co*-PUMA-T) with fluorescent triazene units in structure, the procedure of fluorescence quantification is not applicable due to the very low concentration of triazene fluorophore (around $10^{-9}$–$10^{-10}$ M) in the polymer solution. Therefore, the formation of micelles was further evidenced by adding pyrene ($10^{-6}$ M) in the polymer solution. Considering the highly hydrophobic nature of pyrene molecule, it is expected that in the presence of a hydrophobic phase/microphase such as that found in the micelle core or other macromolecular systems, pyrene to be preferentially solubilized into the interior of the hydrophobic regions of the aggregates.[43,44] The fluorescence spectra of pyrene in aqueous solution were recorded at room temperature, by excitation with $\lambda_{ex} = 320$ nm. Figure 5a shows the fluorescence spectra of pyrene in the PAA-*b*-(PDA-*co*-PUMA-T) solutions, where it can be observed that the monomer (373–410 nm) and excimer (468 nm) fluorescence intensity increases with increasing concentration of polymer. However, the fact that an augmented excimer emission is visible up to high concentrations of polymer, suggests that the micelles formation favours the inclusion of pyrene inside the hydrophobic block in tandem with the reducing of the distance between pyrene molecules. Additionally, the ratio of the emission intensities that appear at 373 nm ($I_1$) and 385 nm ($I_3$) was measured and plotted as a function of the logarithm of PAA-*b*-(PDA-*co*-PUMA-T) concentration (figure 5b). The analysis of the resulting curve profile shows that at low polymer concentration (under $2 \times 10^{-4}$ g $L^{-1}$) the value of $I_1/I_3$ corresponds to a polar medium, when pyrene is exposed to water and

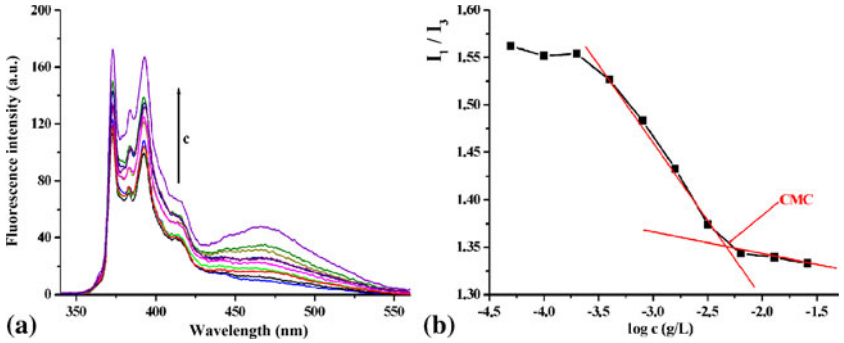


**Figure 5.** Fluorescence spectra of pyrene ($10^{-6}$ M) in aqueous solutions at various concentrations of PAA-*b*-(PDA-*co*-PUMA-T) block copolymer (**a**), plot of the $I_1/I_3$ ratio against concentration of block copolymer (**b**).

the formation of micelles is not visible. However, the value of $I_1/I_3$ decreases up to a constant value at a given polymer concentration ($4 \times 10^{-4}$ g $L^{-1}$). The critical micelle concentration (CMC) was determined from the intersection of straight-line segments, drawn through the points on the rapidly decreasing part of the plot, with that going through the points at the highest polymer concentrations, which lie on a nearly horizontal line. Thus, at high polymer concentration the limiting value of $I_1/I_3$ represents the polarity sensed by pyrene in the hydrophobic sites provided by the polymer micelles. The CMC value of our block copolymer was $4.64 \times 10^{-3}$ g $L^{-1}$ PAA-*b*-(PDA-*co*-PUMA-T) ($3.27 \times 10^{-7}$ M).

From the dynamic light scattering (DLS) measurements, the average size of the particles formed by the block copolymer PAA-*b*-(PDA-*co*-PUMA-T) in aqueous solutions at various concentrations higher than CMC was estimated (figure 6). It was observed that the increase in the polymer concentration from $6.4 \times 10^{-3}$ g $L^{-1}$ to $5.2 \times 10^{-2}$ g $L^{-1}$ determined the enhancement of particles diameter from 154 to 219 nm, accompanied by a narrowing in size distribution (table 1). Also, it can be remarked that the zeta potential of the solutions varied between −40 and −50 mV, showing that the ionic groups were mainly distributed at the surface of the particles and this confirm the good colloidal stability of the resultant solutions.[45]

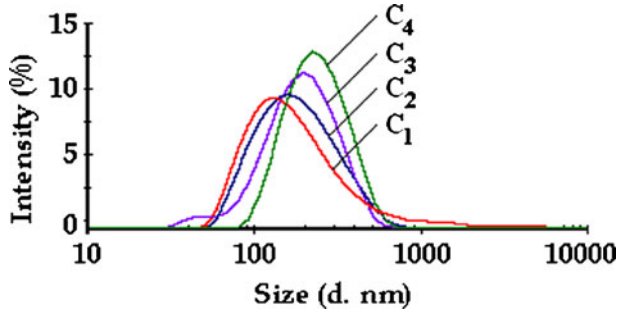


**Figure 6.** Typical size distribution profile for PAA-*b*-(PDA-*co*-PUMA-T) micelles at different concentrations by DLS measurements.

### 3.5 *Quantification of metallic cations by fluorescence measurements*

In the literature, there are only few reports in relation to the quality of the triazene derivatives to act as fluorophores and especially, as chemosensors in the detection of ionic metals.[12,13,46] As a continuation of our work concerning the photochemical performance of some triazene polymers in the development of sensors for metal cations, we investigated some photophysical aspects of the triazene containing block copolymer in DMF solutions and in thin films. When excited at 320 nm, the PAA-*b*-(PDA-*co*-PUMA-T) solution emits a blue fluorescence with well-defined maximum positioned around 400 nm, whereas the maximum of the diblock copolymer in thin film is blue shifted with 25 nm ($\lambda_{em} = 375$ nm).

Firstly, the influence of various metal ions ($UO_2^{2+}$, $Fe^{2+}$, $Fe^{3+}$, $Ni^{2+}$, $Cu^{2+}$, $Co^{2+}$, $Pb^{2+}$ and $Hg^{2+}$) on the fluorescence intensity of the triazene copolymer was followed in DMF solution. It was established that the

**Table 1.** Physicochemical characteristic of the block copolymer micelles determined by DLS.

| Concentration (g $L^{-1}$) | Diameter (nm) | Polydispersity index | Zeta potential (mV) |
|---|---|---|---|
| $6.4 \times 10^{-3}$ | 154 | 0.256 | −40 |
| $1.3 \times 10^{-2}$ | 166 | 0.247 | −41,1 |
| $2.6 \times 10^{-2}$ | 174 | 0.245 | −48,5 |
| $5.2 \times 10^{-2}$ | 219 | 0.170 | −50,1 |

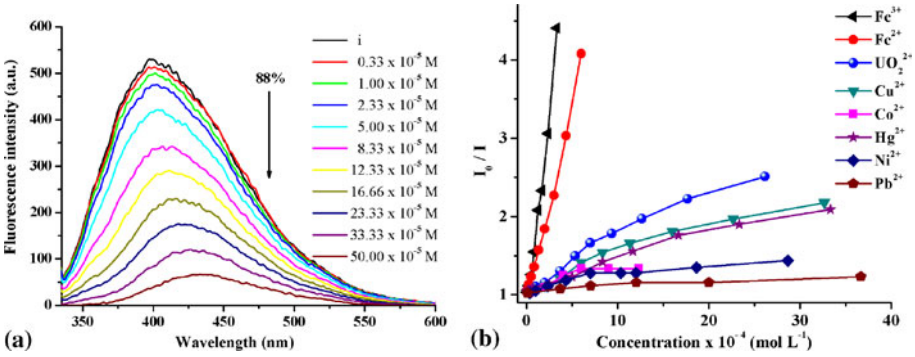


**Figure 7.** Fluorescence spectra of PAA-*b*-(PDA-*co*-PUMA-T) in DMF in the absence and presence of $Fe^{3+}$ at different concentrations (**a**); Stern–Volmer plots for block copolymer in the presence of different metallic cations (**b**); $\lambda_{ex} = 320$ nm.

minimum detectable concentration of $Fe^{2+}$, $Fe^{3+}$, $Pb^{2+}$ and $Hg^{2+}$ cations is around $3.5 \times 10^{-6}$ M. Meanwhile, in the case of the other metallic cations taken in study ($UO_2^{2+}$, $Ni^{2+}$, $Cu^{2+}$, $Co^{2+}$) this parameter is by one order of magnitude higher ($\sim 3.5 \times 10^{-5}$ M). Figure 7a shows the fluorescence intensity changes of PAA-*b*-(PDA-*co*-PUMA-T) excited at $\lambda_{ex}$ = 320 nm, in the presence of $Fe^{3+}$ cations. The fluorescence spectrum of the block copolymer displays a strong emission around 400 nm, which is significantly quenched by the addition of $Fe^{3+}$ ions, hence the presence of $5 \times 10^{-4}$ M $Fe^{3+}$ induced a fluorescence intensity quenching up to 88%. In addition, it can be remarked that the increased levels of quencher cause a batochromic shift of the emission maximum from the initial position 400 nm to 435 nm. An analogous behaviour for the block copolymer solutions was recorded upon addition of $6 \times \cdot 10^{-4}$ M $Fe^{2+}$, $46 \times \cdot 10^{-4}$ M $UO_2^{2+}$ or $49 \times 10^{-4}$ M $Cu^{2+}$, when the fluorescence intensity tends to reach an equilibrium value at about 75.5%, 80% and 63%, respectively. If the quenchers used are $Co^{2+}$, $Hg^{2+}$, $Ni^{2+}$ and $Pb^{2+}$ cations, the florescence intensity of PAA-*b*-(PDA-*co*-PUMA-T) is suppressed at a lower rate, for higher amounts of metallic cations.

The fluorescence quenching efficiency, expressed by the Stern–Volmer constant $K_{sv}$, is determined by monitoring the measurable changes in the fluorescence intensity according to the Stern–Volmer equation [47]

$$I_o/I = 1 + K_{SV}[Q],$$

where $I_o$ and I are the values of fluorescence intensities initial and in the presence of a quencher, respectively, and [Q] is the quencher concentration. The Stern–Volmer plots obtained by the graphical representation of $I_o/I$ as a function of quencher concentration (figure 7b), suggested for our system that the most efficient quenchers are $Fe^{3+}$ ions, followed by the $Fe^{2+}$ cations, whereas the effect of other metal ions ($UO_2^{2+}$, $Cu^{2+}$, $Co^{2+}$, $Hg^{2+}$, $Ni^{2+}$ and $Pb^{2+}$) on the fluorescence decay is less pronounced.

A more explicit quantification of the fluorescence quenching efficiency by metal cations is accessible using the graphical representation of $I_o/I$ ratio, where $I_o$ and I are the values of fluorescence intensities initial and in the presence of a quencher, evaluated at the same quenchers concentration ($5 \times 10^{-4}$ M) (figure 8). Taking into account of the low quencher amount in the measured solutions, it may be noted that the higher degree of fluorescence quenching is obtained for $Fe^{3+}$ and $Fe^{2+}$ ions (of 87.5 and 71.6%, correspondingly), while for the other cations ($UO_2^{2+}$, $Cu^{2+}$, $Co^{2+}$, $Hg^{2+}$, $Ni^{2+}$ and $Pb^{2+}$), the $5 \times 10^{-4}$ M concentrations induced fluorescence quenching below 30%. These experimental results showed that PAA-*b*-(PDA-*co*-PUMA-T) block copolymer displays a high selectivity to iron ions at

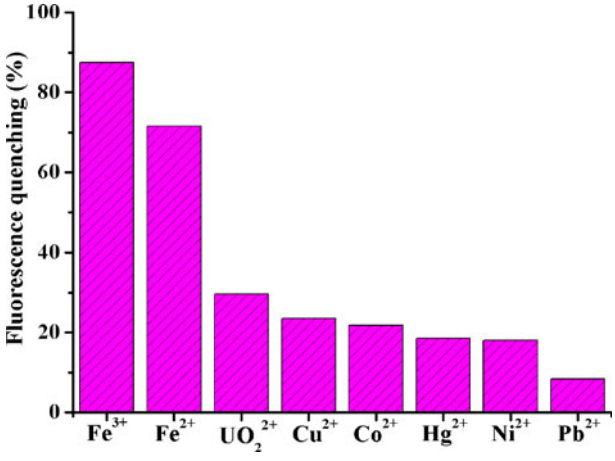


**Figure 8.** Fluorescence quenching degree of PAA-*b*-(PDA-*co*-PUMA-T) in DMF evaluated at quenchers concentration of $5 \times 10^{-4}$ M; $\lambda_{ex} = 320$ nm.

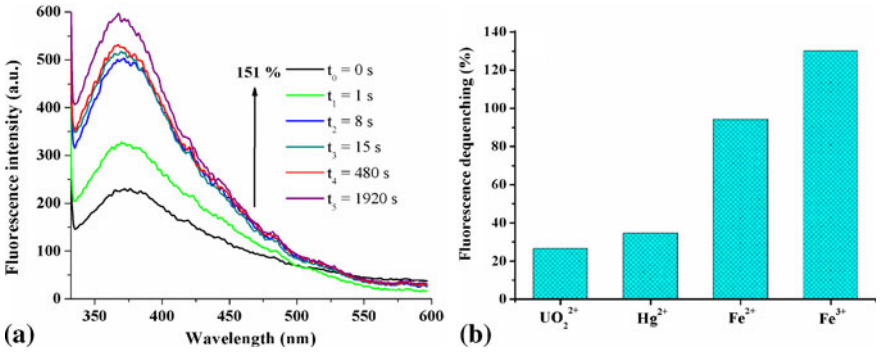


**Figure 9.** Fluorescence spectra of block copolymer films as a function of immersion time in deionized water containing $1 \times 10^{-6}$ M $Fe^{2+}$ ions (**a**); fluorescence increase for block copolymer film after 900 s exposure in deionized water containing various metallic cation solutions ($10^{-6}$ M) (**b**).

very low concentrations of quencher (in the range of $10^{-5}$ M).

Finally, the fluorescence emission of block copolymer PAA-*b*-(PDA-*co*-PUMA-T) in thin film was studied in the presence of some quenchers dissolved into aqueous solution at a concentration of about $10^{-6}$ M. Compared with polymer solution, the PAA-*b*-(PDA-*co*-PUMA-T) film illustrates large fluorescence enhancements after different times of exposure to aqueous media containing $Fe^{3+}$ cations (figure 9a). Thus, after 1920 s of film exposure to $Fe^{3+}$ cation solutions, an augmentation of fluorescence intensity with about 151% is observed, whereas $Fe^{2+}$ cations produced a fluorescence intensification of 97.8% for the same time. In similar conditions, the use of uranyl and mercury metal cations generates a modest increase of fluorescence (39.3% and 34.6%, respectively). In all situations, the minimum detection time was 1 s, but after 900 s, the fluorescence intensity was amplified in variable proportions, as shown in figure 9b.

Therefore, it should be emphasized that the triazene sequences from PAA-*b*-(PDA-*co*-PUMA-T) block copolymer are very sensitive to iron cations, especially when the polymer is in film state, since after a period of contact of 1 s with the analyte solution, the fluorescence intensity was enhanced with about 42%. Hence, this approach will allow in the future the design of efficient structures for the selective detection of $Fe^{3+}$ from chemical or biological environments.

## 4. Conclusions

A novel block copolymer with the poly(acrylic acid) hydrophilic block and the hydrophobic block containing dodecylacrylamide and triazene units was prepared by the microwave accelerated RAFT technique. The investigation of the thermal and morphological characteristics for macroPAA (macro-RAFT agent) and the formed block copolymer showed that these polymers display an adequate thermal stability for the envisioned applications (they are thermally stable up to 160°C), while the morphological analysis revealed a homogeneous morphology of the polymer surface. The photolability study of the triazene structure enclosed in the block copolymer under UV irradiation, demonstrated that the photolysis reactions proceeds following a first-order kinetic model, being significantly influenced by the solvent polarity. The ability of block copolymer to form micelles in water was proved through fluorescence measurements using pyrene as a probe, the determined critical micelle concentration value being of $3.27 \times 10^{-7}$ M PAA-*b*-(PDA-*co*-PUMA-T). The average sizes of the micelles formed at various concentrations of PAA-*b*-(PDA-*co*-PUMA-T) were estimated by DLS measurements, and values between 154 and 219 nm were found out. The fluorescence study demonstrates the potential of the block copolymer with triazene pendant to function as chemosensor for metal ions in organic medium and in film state, with a significant role in the detection of heavy metals.

## Acknowledgements

The authors (TB and VM) are thankful for the financial support offered by European Social Fund – "Cristofor I Simionescu" Postdoctoral Fellowship Programme (ID POSDRU/89/1.5/S/55216), Sectoral Operational Programme Human Resources Development 2007–2013.

## References

1. Moon J H and Yang S 2010 *Chem. Rev.* **110** 547

2. Yu H, Naka Y, Shishido A and Ikeda T 2008 *Macromolecules* **41** 7959
3. Angiolini L, Benelli T, Giorgini L, Mauriello F and Salatelli E 2006 *Macromol. Chem. Phys.* **207** 1805
4. Ito H 2005 *Adv. Polym. Sci.* **172** 37
5. Hoogen N and Nuyken O 2000 *J. Polym. Sci. Part A: Polym. Chem.* **38** 1903
6. Nuyken O, Dahn U, Wokaun A, Kunz T, Hahn C, Hessel V and Landsiedel J 1998 *Acta. Polym.* **49** 427
7. Nagel M, Hany R, Lippert T, Molberg M, Nuesch F A and Rentsch D 2007 *Macromol. Chem. Phys.* **208** 277
8. Buruiana E C, Melinte V, Buruiana T and Simionescu B C 2005 *J. Appl. Polym. Sci.* **96** 385
9. Buruiana E C, Melinte V, Buruiana T, Lippert T, Yoshikawa H and Mashuhara H 2005 *J. Photochem. Photobiol. A: Chem.* **171** 261
10. Buruiana E C, Buruiana T, Hahui L, Lippert T, Urech L and Wokaun A 2006 *J. Polym. Sci. Part A: Polym. Chem.* **44** 5271
11. Buruiana E C, Melinte V, Buruiana T and Simionescu B C 2008 *Des. Monom. Polym.* **11** 423
12. Buruiana E C, Stroea L and Buruiana T 2009 *Polym. J.* **41** 694
13. Melinte V, Buruiana T, Tampu D and Buruiana E C 2011 *Polym. Int.* **60** 102
14. Perrier S and Takolpuckdee P 2005 *J. Polym. Sci. Part A: Polym. Chem.* **43** 5347
15. Barner-Kowollik C and Perrier S 2008 *J. Polym. Sci. Part A: Polym. Chem.* **46** 5715
16. Moad G, Rizzardo E and Thang S H 2009 *Aust. J. Chem.* **62** 1402
17. Lowe A B and McCormick C L 2007 *Prog. Polym. Sci.* **32** 283
18. Chong B Y K, Le T P T, Moad G, Rizzardo E and Thang S H 1999 *Macromolecules* **32** 2071
19. Garnier S and Laschewsky A 2006 *Colloid Polym. Sci.* **284** 1243
20. Cui Q, Wu F and Wang E 2011 *Polymer* **52** 1755
21. Schilli C M, Zhang M, Rizzardo E, Thang S H, Chong Y K, Edwards K, Karlsson G and Muller A H E 2004 *Macromolecules* **37** 7861
22. Zhang W, Zhang W, Zhou N, Cheng Z, Zhu J and Zhu X 2008 *Polymer* **49** 4569
23. Lazzari M, Liu G and Lecommandoux S 2006 *Block copolymers in nanoscience*. Weinheim: Wiley VCH
24. Kita-Tokarczyk K, Grumelard J, Haefele T and Meier W 2005 *Polymer* **46** 3540
25. Olsen B D and Segalman R A 2008 *Mater. Sci. Eng. R: Reports* **62** 37
26. Li M H and Keller P 2009 *Soft Matter* **5** 927
27. Kwon G S and Forrest M L 2006 *Drug Dev. Res.* **67** 15
28. Osada K, Christie R J and Kataoka K 2009 *J. R. Soc. Interface* **6** S325
29. Huang M H, Li S and Vert M 2004 *Polymer* **45** 8675
30. Kappe C O, Dallinger D and Murphree S 2009 *Practical microwave synthesis for organic chemists.* Weinheim: Wiley VCH
31. Kappe C O 2004 *Angew. Chem. Int. Ed.* **43** 6250
32. Polshettiwar V, Nadagouda M N and Varma R S 2009 *Aust. J. Chem.* **62** 16
33. Roy D, Ullah A and Sumerlin B S 2009 *Macromolecules* **42** 7701
34. Kempe K, Becer C R and Schubert U S 2011 *Macromolecules* **44** 5825
35. Zetterlund P B and Perrier S 2011 *Macromolecules* **44** 1340
36. Brown S L, Rayner C M, Graham S, Cooper A, Rannard S and Perrier S 2007 *Chem. Commun.* **21** 2145
37. Buruiana E C, Chibac A L and Buruiana T 2010 *J. Photochem. Photobiol. Part A: Chem.* **213** 107
38. Chong Y K, Krstina J, Le T P T, Moad G, Postma A, Rizzardo E and Thang S H 2003 *Macromolecules* **36** 2256
39. Buruiana E C, Melinte V, Buruiana T, Simionescu B C, Lippert T and Urech L 2007 *J. Photochem. Photobiol. A: Chem.* **186** 270
40. Alexandridis P and Lindman B 2000 *Amphiphilic block copolymers. Self-assembly and applications*. Amsterdam: Elsevier Science
41. Lu X, Gong S, Meng L, Li C, Liang F, Wu Z and Zhang L 2007 *Eur. Polym. J.* **43** 2891
42. Olea A F, Silva P, Fuentes I, Martínez F and Worrall D R 2011 *J. Photochem. Photobiol. A: Chem.* **217** 49
43. Turro N J, Gratzel M and Braun A 1980 *Angew. Chem. Int. Ed.* **19** 675
44. Prochazka K, Vajda S, Fidler V, Bednar B, Mukhtar E, Almgren M and Holmes S 1990 *J. Mol. Struct.* **219** 377
45. Liu Y-Y, Su X, Tang M-F and Kong J 2007 *Macromol. Chem. Phys.* **208** 415
46. Ressalan S and Iyer C S P 2005 *J. Lumin.* **111** 121
47. Lakowicz J R 2006 *Principles of fluorescence spectroscopy,* 3rd ed. New York: Springer Science and Business Media LLC